Fluorocarbon vapors slow down coalescence in foams: influence of surfactant concentration

Katja Steck, Jonathan Dijoux, Natalie Preisig, Victor Bouylout, Cosima Stubenrauch, Wiebke Drenckhan-Andreatta

Fluorocarbon Vapors Slow Down Coalescence in Foams: Influence of Surfactant Concentration

Katja Steck[1], Jonathan Dijoux[1], Natalie Preisig[2], Victor Bouylout[1], Cosima Stubenrauch[2], Wiebke Drenckhan[1]

[1]Institut Charles Sadron, University of Strasbourg, CNRS UPR22, 23 Rue du Loess, 67037 Strasbourg, France

[2]Institute of Physical Chemistry, University of Stuttgart, Pfaffenwaldring 55, 70569 Stuttgart, Germany

Abstract

Even though it has been known for a long time that traces of perfluorinated vapors suppress gas exchange (coarsening) between the bubbles of aqueous foams, its stabilizing impact on foam coalescence has been evidenced only recently. While previous work has demonstrated this effect for different surfactant types, we investigate here the influence of the surfactant concentration. We compared the foam properties of aqueous solutions of the non-ionic surfactant dodecyldimethylphospine oxide (C_{12}DMPO) in the absence and presence of perfluorohexane (PFH) in the gas phase. In order to decouple foam coarsening and coalescence, we accompany the foam stability experiments with (a) lifetime statistics of individual, vertical foam films pulled from the same solutions and (b) surface tension measurements in controlled gas environments. All measurements show a clear increase of foam and film stability in the presence of PFH, its effect being most pronounced above the cmc of the surfactant. The surface tension measurements show a clear co-adsorption of the PFH up to the formation of macroscopic films at saturation. We complete the analysis by showing that alkane vapors also have a stabilizing effect for the same surfactant solutions, yet much less pronounced than that of PFH. The precise origin of the stabilizing action of these hydrophobic vapors remains to be elucidated.

1. Introduction

Tuning the stability of liquid foams is one of the major challenges to optimize their use for specific applications (i.e. medicine, cosmetics, cleaning, food and beverages or as templates for solid foams).[1–4] Destabilization occurs by (1) gravity-driven *drainage* of liquid, (2) *coalescence* (film rupture), and (3) *coarsening* (gas transport). Different routes to control the stability of foams have been developed.[1–4] One example is the use of fluorocarbon (FC) vapors to reduce coarsening.[1,4] The poor water solubility of FCs inhibits their transport across the liquid films of the foam, which leads to an osmotic pressure drop counterbalancing the Laplace pressure, i.e. the driving force of coarsening.[5,6] However, we recently showed that FC vapors, even at low concentrations, also effectively slow down coalescence in foams and that this effect occurs for a wide range of surfactant types, such as non-ionic polyethylene glycols (including fluorinated ones – S1 in SI), phosphine oxides and silicone-based block copolymers[7]. The FC vapor acts thereby as co-adsorbate from the gas phase[7] which was revealed by surface tension measurements. The co-adsorption of surfactants and FC vapors at interfaces had already been studied for non-ionic as well as cationic surfactants[8], proteins and phospholipids[9–12]. Our measurements confirmed that (i) the surfactant and the FC co-adsorb at the interface forming a mixed monolayer at low FC concentrations, followed by (ii) continuous adsorption with increasing FC concentration, until (iii) a macroscopic FC film forms if the gas phase is saturated with FC.[7] Similar interfacial behavior was put in evidence for cationic, non-ionic as well as anionic surfactants and different oil vapors, i.e. mainly alkane vapors[13–15], but also a silicone oil and an FC vapor[13].

Whereas the influence of FC vapors (and also alkane vapors) on interfaces[8,10,14,16–20] has been studied extensively, only little is known about their influence on foam properties. In particular, a reliable quantification remains a major challenge. Even their impact on coarsening, for which the role of FC vapors is well-known, has only little been investigated quantitatively[21]. In the case of coalescence, we were the first to link its slowing down to the presence of the FC vapors in foams. For alkanes, Binks e*t al*.[22] were the first to report on their influence on coalescence in foams. However, they found a contradictory behavior to our observations with FC vapors, i.e. the foam stability was reduced in the presence of the oil vapors.

In order to gain a more fundamental understanding of the influence of FC vapors (here: perfluorohexane) on the slowing down of coalescence in foams, we decided to investigate the role of the surfactant concentration. We chose to study foams of aqueous solutions of dodecyldimethylphospine oxide (C_{12}DMPO) below and above the cmc because the foams are highly unstable. We showed in our previous work[7] that the dominant ageing mechanism in highly unstable foams is coalescence (rather than coarsening), and that coalescence is slowed down in the presence of perfluorohexane. Foam stability measurements (Section 3.1), accompanied by surface tension measurements (Section 3.2), allow us to deduce how the ability of perfluorohexane to slow down coalescence is linked to the interfacial behavior for different surfactant concentrations. Since foam stability is governed by several, interlinked phenomena, we complement the foam experiments by lifetime measurements of individual, vertical thin films pulled from the surfactant solution with and without perfluorohexane in the gas phase (Section 3.3). These experiments allow

us to investigate the influence of perfluorohexane on the free drainage and lifetime of individual films.

Last but not least, to compare with the contrasting work by Binks *et al.*[22], we investigate the influence of an alkane vapor (here: hexane) at different concentrations on the coalescence of foams of an aqueous C_{12}DMPO solution at 10 cmc. The similar interfacial behavior of the two vapors suggests a similar behavior in foams (Section 3.4).

2. Materials and Methods

2.1 Materials and Sample Preparation

Aqueous solutions of the non-ionic surfactant C_{12}DMPO were prepared at different surfactant concentrations c = x *cmc* with *cmc* = $3.0 \cdot 10^{-4}$ M (Section 3.2) and M = 246.37 g/mol using Milli-Q water. C_{12}DMPO, perfluorohexane and hexane were purchased from ABCR chemicals, Sigma Aldrich and Carlo Erba, respectively, and used without further purification. NaCl ($c_{NaCl} = 10^{-2}$ M) is added to the solutions for the foam experiments (see Section 2.2). NaCl was roasted overnight at T = 500 °C to remove organic contaminants.

2.2 Foaming Experiments

The foams were characterized by conductivity measurements and image analysis with the commercially available *FoamScan* (http://teclis.eu). Note that for these experiments, sodium chloride ($c_{NaCl} = 10^{-2}$ M) was added to the surfactant solutions. NaCl at these concentrations does not affect foam properties[23], but ensures the conductivity of the solution in order to measure the liquid fraction (liquid volume divided by foam volume). Using a syringe pump from Harvard Apparatus, a mixture of air and perfluorohexane was pumped through a porous glass frit of porosity R_f = 20-50 µm (P2) into the foaming solution contained in the *FoamScan* column. The perfluorohexane concentration in the gas was set by controlling the partial pressure p of perfluorohexane in air with respect to its vapor pressure p_0 (taken to be 24 kPa at 20 °C[24]). Different ratios of p/p_0 were adjusted by adding different volumes of liquid perfluorohexane to 60 mL syringes already filled with 50 mL of air at atmospheric pressure (taken to be 10^5 Pa; calculated according to[21]) An error of 5% is estimated. All foams were generated at room temperature (T = 20 ± 1 °C) with a total gas volume of 100 mL and a total gas flow rate of 80 mL min^{-1}. The column was closed with *Parafilm* in order to minimize the osmotic pressure difference with the exterior. This would otherwise lead to a net gas transport into the foam with time, i.e. to its growth[25]. Only a small hole was left in the cover to allow for pressure equilibration. The first measurement was performed to ensure equilibrium conditions while the results of the second to fourth measurements were averaged for foam height and bubble size distributions. As shown in our previous publication[7], these measurements are highly reproducible. How the mean bubble radius can be derived from the measurements has been explained in detail by Boos *et al.*[23]

2.3 Surface Tension Measurements

The surface tension of the foaming solutions was measured at room temperature (T = 20 ± 1 °C) as a function of the surfactant concentration with the *Tracker* from Teclis. A 3 µL rising bubble is created on a syringe needle in a 25 mL surfactant solution. The gas mixtures were prepared as described in Section 2.2. For each surface tension measurement, a series of 4 bubbles was recorded. The first bubble ensured equilibration of the system and the results of the following three bubbles were averaged to calculate the surface tension. The spread of the data gives an average deviation of ± 0.2 mNm^{-1} for the surface tension.

The interfacial tension between liquid PFH and the surfactant solution at a concentration above the cmc (c = 10^{-3} M) was measured with *Profile Analysis Tensiometer PAT-1* from Sinterface Technologies.

2.4 Film Pulling Device

Lifetimes of vertical thin films of aqueous solutions of C_{12}DMPO in the absence and presence of PFH were determined with a home-made film pulling device contained in a square box of volume V_{box} = 15 625 cm^3. In this experiment, a frame of dimension 6 cm x 0.5 cm x 5 cm contains a network of nylon fishing lines 0.15 mm thickness creating a rectangular zone of 2 x 3 cm in which the films were formed by pulling the frame from the surfactant solution. The frame is held by an arm attached to a motor which pulls it out of the soap solution automatically and at controlled speed. For the measurements presented in this publication, the frame was immersed into a cuvette of volume $V_{cuvette}$ = 7 cm x 1 cm x 9 cm at velocity v = 50 mm/s and acceleration a = 100 mm/s^2 and subsequently pulled out at v = 100 mm/s and a = 200 mm/s^2. The film drainage is visualized by recording the interference pattern of white light reflected from the film using a diffusive light panel (Godox ES45 E-Sport LED Light Kit) and a digital camera (IDS U3-3800CP-C-HQ). The breaking times were automatically saved as soon as film breaking was detected by the camera, i.e. as soon as a previously defined intensity threshold of light reflected from the film was reached. As soon as the film broke, it was re-created by repeating the procedure. Each measurement was repeated 200 times. The measurements were performed at room temperature and at controlled relative humidity at the beginning of the measurements. The latter was set to RH = 75 % by placing a saturated salt solution (NaCl)[26] into the measuring chamber overnight. For the measurements with perfluorohexane (PFH), 20 mL of liquid PFH were inserted into a small petri dish in the chamber through a small opening using a syringe and left to evaporate.

The relative humidity is an important factor in these measurements since it is known to be a determining factor regarding foam film stability[27]. Figure 1a shows the evolution of the relative humidity with increasing number of pulled films at 10 cmc in the absence and presence of PFH. For the measurements with air only, the relative humidity increases from the previously set RH = 75 % up to a plateau at $RH \approx$ 80-85%. This increase is due to water evaporation from the films. In contrast, as soon as liquid PFH is added to the measuring chamber, the relative humidity decreases, reaches a minimum ($RH \approx$ 75%) and increases again. The decrease of the relative humidity is a consequence of the continuous evaporation of PFH after its insertion to the device. The pressure in the chamber is the sum of the partial pressures of the gases present according to Dalton's Law.

Assuming a constant pressure $p \approx p_{atm}$ since the chamber is not completely sealed, the evaporation of PFH leads to a finite partial pressure p_{PFH} in the gas phase and thus a decreasing partial pressure of water p_{water}, i.e. a lower relative humidity. Full evaporation of the liquid PFH means in our experiment the highest possible p_{PFH} and thus the lowest relative humidity. This is reflected by the minimum of the relative humidity with increasing number of pulled films in the presence of PFH. Since the chamber is not perfectly sealed, the PFH diffuses out which leads to a subsequent increase of the relative humidity. Figure 1b shows one example of the film lifetimes measured during this evolution. In the absence of PFH, the film lifetimes are in the range of 40 – 70 s, whereas the film lifetimes with PFH are much more scattered. Immediately after the addition of PFH, i.e. PFH is not fully evaporated, the film lifetimes are initially lower than those obtained with air only – which is probably due to the decreased humidity leading to faster evaporation of water. However, at the highest possible PFH concentration, i.e. at minimum *RH*, the film lifetimes are strongly increased (70 – 140 s) and are thus higher than those for air only. After PFH starts to evaporate out of the film pulling chamber, the vertical film lifetimes decrease again to lower levels than those with air only. For all further comparison we systematically chose the 40 films generated around the minimum *RH* value (see dashed rectangle in Figure 1) such that we can ensure the maximal presence of PFH.

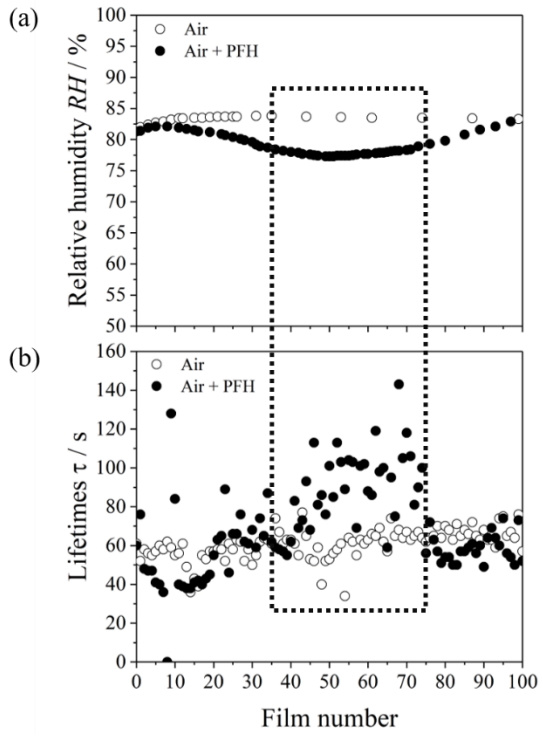

Figure 1: (a) Example of the evolution of relative humidity *RH* in the measurement chamber during the measurements and (b) lifetime τ of vertical thin liquid films of an aqueous C_{12}DMPO solution at a concentration of c = 10 cmc using a film pulling device in the absence and the presence of perfluorohexane (PFH) in the measuring chamber.

3. Results

3.1 Foam Stability

In Figures 2 and 3, photographs of foams of aqueous solutions of C_{12}DMPO at different concentrations, foamed with (i) air and (ii) air + perfluorohexane (PFH), show the time evolution of the foam height and the bubble size, respectively. In Figure 4 the measured foam height *h* (Figure 4a) and the mean bubble radius $\langle r \rangle$ (Figure 4b) are plotted as a function of time. For the foams formed with air only (Figure 2 top), one sees that they become more transparent within the first 300 s after foam generation and already collapse to half their height (0.5 and 10 cmc) or start to collapse (1, 2, and 5 cmc) (Figure 4a). The increasing transparency is due to an increasing bubble size, in line with Figure 2 and 3b. After 1000 s, the foams are almost fully collapsed for all C_{12}DMPO concentration. In contrast, the foams formed with traces of perfluorohexane (PFH) are much more stable. Whereas the foams below the cmc show degradation after 300 s (increasing transparency, decreasing foam height), those above the cmc are stable up to 1000 s.
The bubble size evolution shown in Figure 3 confirms the macroscopic foam observations. The mean bubble radius $\langle r \rangle$ obtained from these images is plotted vs time in Figure 4b. Here we focus only on the first 300 s after foam generation since we can ensure that the foam degradation is dominated by coalescence within this time range.[7] For both, the foams formed without and with PFH, the initial bubble size depends slightly on the surfactant concentration, i.e. it is smaller above the cmc than below. On the one hand, this is related to the higher surface tension below the cmc, leading to gravity-driven bubble detachment from the porous frit at larger bubble size. On the other hand, this is a result of the lower foam stability, leading to bubble coalescence already during the foaming process.
When the foams are formed with air only, the bubble size rapidly increases within 180 s after foam production. Above the CMC, this increase seems independent of the surfactant concentration. The rapid increase accompanied by the collapse of the foams is characteristic for coalescence. For the foams formed with traces of PFH, however, the surfactant concentration has a measurable influence on the evolution of the bubble size. For a surfactant concentration of 0.5 cmc, the bubble size rapidly increases over the first 300 s after foam production. At cmc and 2 cmc, the bubble size marginally increases within the first 180 s after foam production but then remains constant. For 5 cmc and 10 cmc, the bubble size remains constant in the given time range.

In summary, one can conclude that the slowing down of coalescence by PFH vapors depends on the surfactant concentration. Below the cmc, i.e. at 0.5 cmc, the effect is small, shown by the rapid increase of the bubble size. For surfactant concentrations close to the cmc (1, 2 cmc), coalescence is already significantly slowed down by the presence of PFH. At 5 cmc and 10 cmc, the slowing down of coalescence by PFH is most pronounced, i.e. it seems that the PFH needs a densely packed surfactant monolayer to be fully effective.

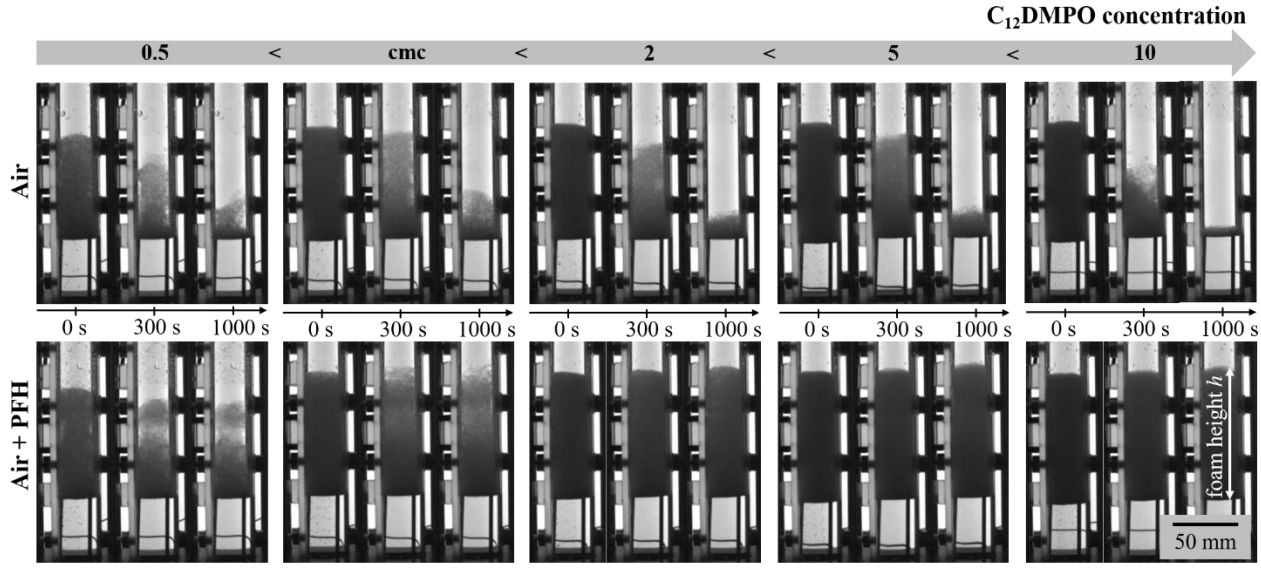

Figure 2: Photographs of foams of aqueous C_{12}DMPO solutions at concentrations of c = 0.5, 1, 2, 5, 10 cmc with and without perfluorohexane (PFH) in the foaming gas (air) obtained from *FoamScan* measurements. The amount of PFH, i.e. the ratio of partial pressure p of perfluorohexane to its vapor pressure p_0, was set to p/p_0 = 0.15.

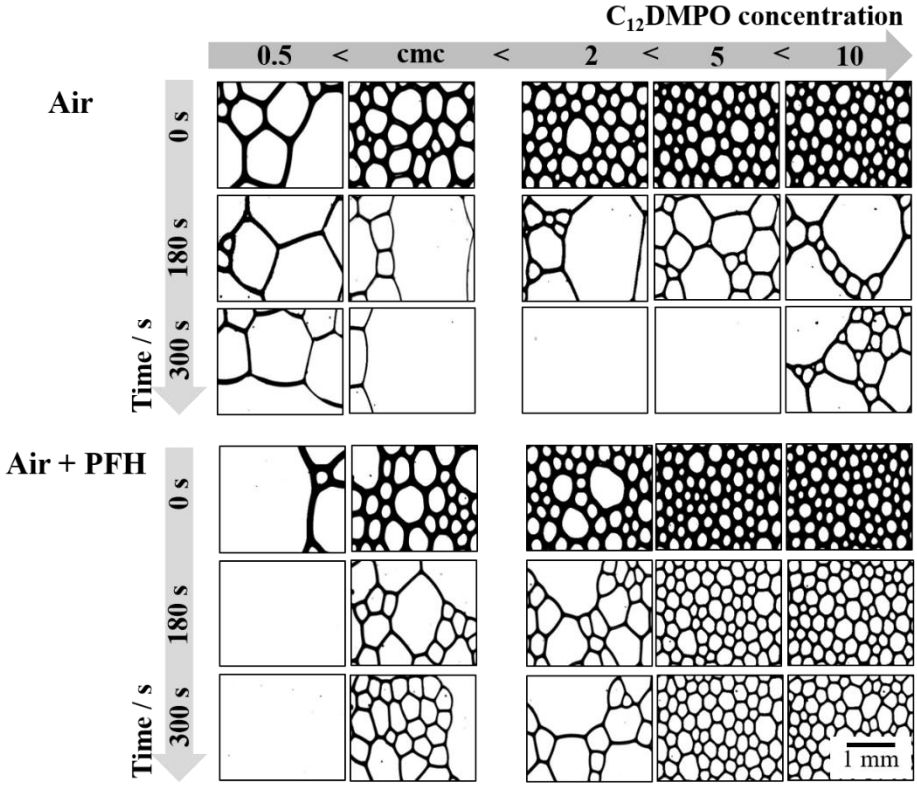

Figure 3: Close-up photographs showing the bubble size evolution of the foams of aqueous C_{12}DMPO solutions of Figure 2.

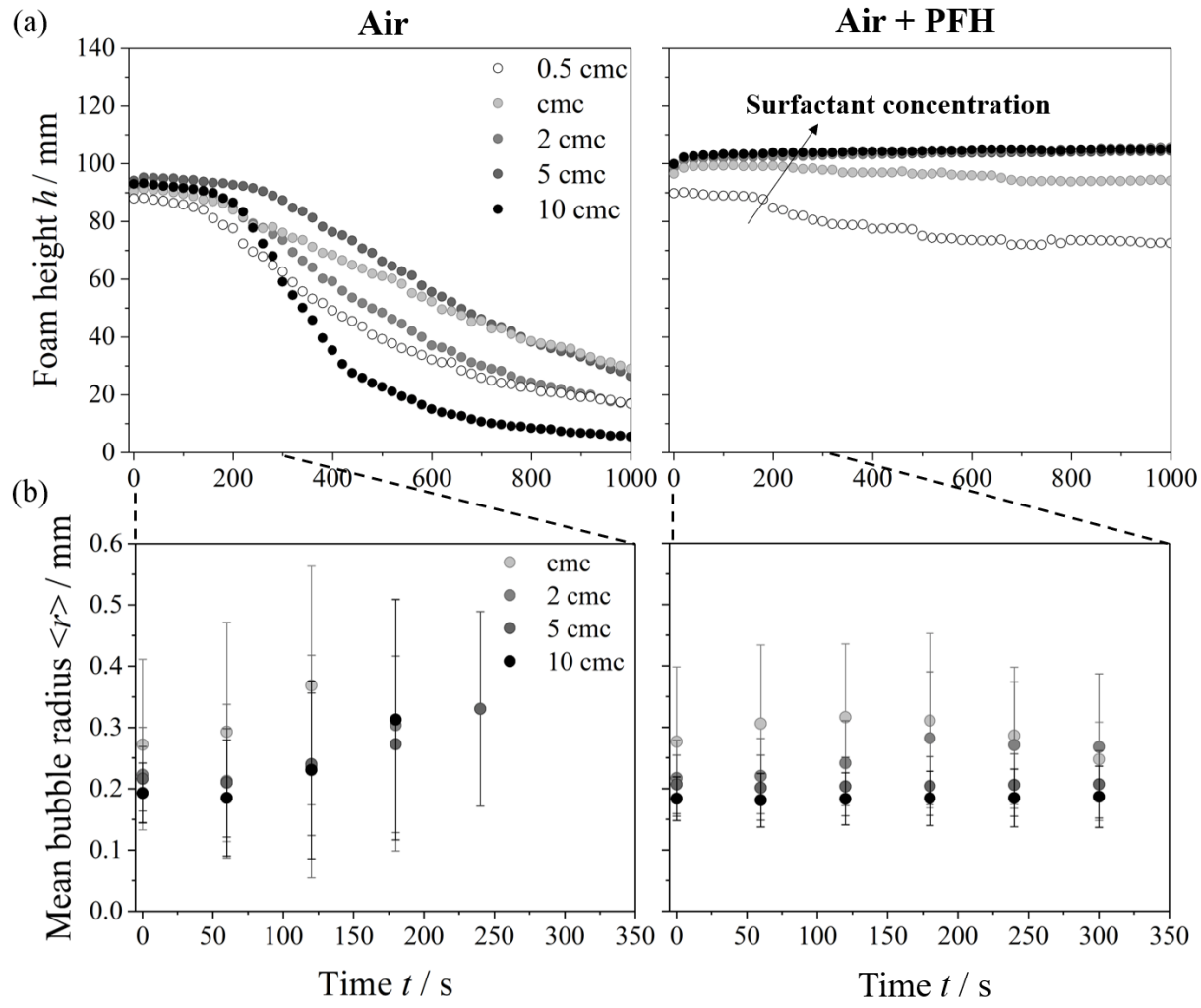

Figure 4: (a) Foam height h and (b) mean bubble radius $\langle r \rangle$ versus time t for foams of aqueous C_{12}DMPO solutions at different concentrations c = 0.5, 1, 2, 5 and 10 c*mc* shown in Figure 2 and 3.

3.2 Surface tension measurements

In order to understand the influence of the surfactant concentration on the ability of PFH to reduce coalescence, we performed surface tension measurements. Figure 5 shows the equilibrium surface tension versus the C_{12}DMPO concentration in the absence (white circles) and presence of PFH at p/p_0 = 1.0 (black circles) in the gas phase. In line with the literature[7,14,16,17], the surface tension decreases to lower values in the presence of PFH due to the co-adsorption of the surfactant and the PFH molecules. As was discussed by Miller and collaborators[18,28–30] in the case of alkanes or fluorocarbons at p/p_0 = 1.0, the hydrophobic vapor is expected to form multi-layers at the interface, as sketched in Figure 5. We showed in our previous work, in line with results presented by Binks *et al.*[13], that the created film behaves like a macroscopic film. In other words, as sketched in

Figure 5V, the total "effective surface tension γ_{eff} " of the complex interface is equal to the sum of (1) the surface tension between air and PFH ($\gamma_{air/PFH}$ = 13 mN/m[31]) and (2) the interfacial tension between PFH and the surfactant solution, which we measured to be $\gamma_{sol/PFH}$ = 9.7 ± 0.2 mN/m above the cmc. The sum $\gamma_{air/PFH}$ + $\gamma_{sol/PFH}$ gives 22.7 mN/m which is very close to the value of γ_{eff} = 23 ± 0.5 mN/m measured by us above the cmc. This means, that the PFH film is thick enough so that the two interfaces can be considered independent.

Figure 5 shows that this co-adsorption also leads to a slight shift of the cmc. For the system without PFH, the cmc of C_{12}DMPO is $3.0 \cdot 10^{-4}$ M, whereas this value increases to $4.6 \cdot 10^{-4}$ M with PFH. While the precise value of this shift needs to be taken with care due to the few data points we have for the surface tension with PFH, there is no doubt that such a shift is present. At first glance, this seems surprising, since the PFH is not soluble in water and should therefore not have an influence on the cmc of the surfactant, which is a bulk property. Such a shift may potentially be explained by the interactions between the surfactants and the PFH at the interface changing their chemical potential.

We fit the surface tension data below the cmc (Figure 5) with a second order polynomial function $f = \gamma(\ln c)$[32,33] to calculate the surface excess concentration Γ and the area per surfactant molecule A on the surface. Using the Gibbs adsorption isotherm

$$\Gamma(c) = -\frac{1}{RT}\left(\frac{d\gamma}{d\ln c}\right)_{p,T} \quad (1)$$

and $$A = \frac{1}{N_A \Gamma_{max}} \quad (2)$$

(with γ – equilibrium surface tension, c – surfactant concentration, $\Gamma_{max} = \Gamma$(cmc), R – gas constant, N_A – Avogadro constant and T – temperature), we find that without PFH, a surfactant molecule takes up 40 ± 2 Å^2 on average at the cmc. If we make the assumption that the influence of the PFH on the chemical potential of the surfactant at the interface can be neglected, we can use the same procedure on the data in the presence of PFH to obtain 56 ± 3 Å^2 surface area per surfactant molecule. This could indicate that the co-adsorption of both species increases the area taken up by each surfactant molecule. However, as discussed before, since we are dealing here with a macroscopic PFH film, the Gibbs adsorption isotherm is likely not applicable and one needs to turn instead to more complex modeling[28,30]. This is discussed in more detail in Section 4.

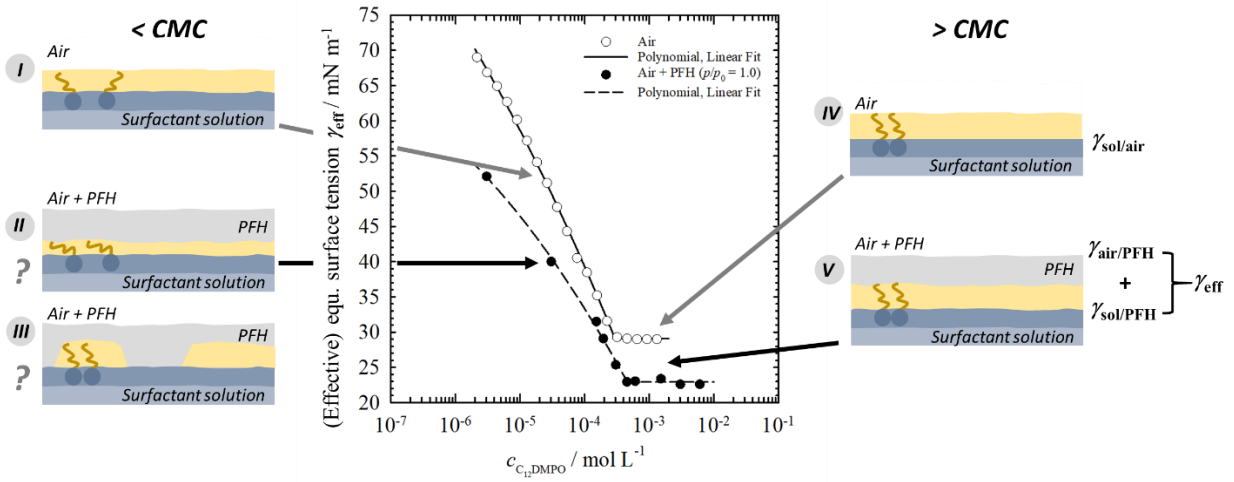

Figure 5: Equilibrium surface tension versus C_{12}DMPO concentration in the absence (white circles[34]) and presence of PFH at p/p_0 = 1.0 (black circles) in the gas phase. Sketched are potential configurations of the interface below (I-III) and above (IV) the CMC in the absence (I,IV) or presence (II,III,V) of PFH at p/p_0 = 1.0.

3.3 Investigations of individual foam films

Investigating coalescence in foams is a challenge, since the different ageing mechanisms (see Section 1) are coupled. In particular, it is difficult to exclude fully the potential influence of coarsening, which is stopped in the presence of PFH. For a better understanding on how PFH impacts the coalescence of foam films, we therefore studied the drainage and rupture of individual, vertical foam films of C_{12}DMPO solutions in the absence and presence of PFH. Figure 6 shows photographs of the evolution of two representative vertical films at 10 cmc formed in the absence and presence of PFH, respectively. The evolution of films made by two different C_{12}DMPO concentrations (0.5 and 2 cmc) are given in the Supporting Information (Figure S2 and S3). In addition, a color code is given (Figure 6a) which connects the colors that occur in a draining vertical thin film to its thickness. Details of how this color map is obtained are given by Andrieux *et al.*[35]

Directly after the films were pulled out (t = 0 s), no clear color can be identified, i.e. the film is thicker than 1000 nm. Within the first 40 s, different colors occur indicating film thinning due to gravity-driven drainage. Comparing the visual evolution of the films, PFH seems to have no measurable influence on their initial drainage. In both cases, i.e. with or without PFH present, the center of the films drains to thicknesses around 400 nm after 20 s and 200 nm after 40 s. At 40 s a Newton Black film ("NBF", film thickness < 10 nm) starts to occur at the top of the film indicated by the black areas. This NBF corresponds to a hydrated surfactant bi-layer which forms spontaneously in films stabilized by C_{12}DMPO well above the cmc and drained sufficiently[36]. At longer film lifetimes (≥ 60 s), the influence of PFH becomes substantial. For the films formed in absence of PFH, the area of the NBFs grows faster than for those formed in the presence of PFH. At this stage, the evaporation of water from the film determines the vertical thin film stability[27].

This seems to be slowed down by the presence of PFH since the zone of the NBF increases more slowly. Moreover, larger zones of NBF are reached (see 104 s) before the film breaks indicating a higher stability of NBFs in the presence of PFH. Thus, not only the formation of the NBFs is slowed down due a lower water evaporation, but also the NBFs itself are stabilized by the presence of PFH. Both, slower NBF formation and increased stability lead to a longer film lifetime.

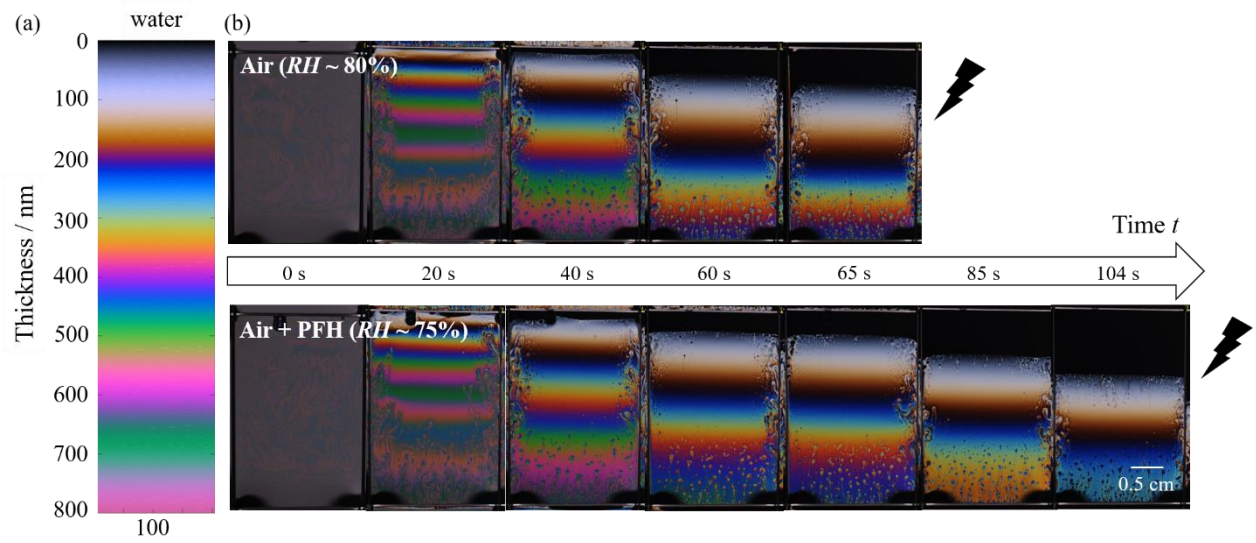

Figure 6: (a) Color code relating the color to the thickness of a thin film of an aqueous solution created by white light interference. (b) Photographs showing the evolution of draining vertical foam films of an aqueous C_{12}DMPO solution at 10 cmc in the absence (top) and presence (bottom) of PFH in the measuring chamber of the film pulling device with relative humidity *RH*. The *RH* values are slightly different, as explained in Section 2.4.

To study the influence of the C_{12}DMPO concentration on the film lifetime, we do full lifetime statistics for the film measurements, i.e. we measure the lifetime of at least 40 films for each formulation with and without PFH. In Figure 7 the film lifetimes at all concentrations in the absence (left) and presence (right) of PFH are compared by means of a box plot. For the films formed in air only, one sees that the surfactant concentration has an influence on the film lifetime: Up to the cmc, here at 0.5 and 1 cmc, average film lifetimes of $\tau \sim 20$ s and $\tau \sim 40$ s, respectively, are reached. I.e. film lifetimes increase with increasing surfactant concentration. Above the cmc, film lifetimes are longer than below the cmc. Average lifetime values of $\tau \sim 60$ s are reached at 2, 5 and 10 cmc showing no measurable influence of the surfactant concentration on film stability above the cmc. In addition, the scatter in lifetime is much narrower above the cmc than below.

In the presence of PFH, the film lifetimes show overall the same dependence on surfactant concentration. Up to the cmc, the average lifetimes increase with increasing surfactant concentration and reach values of $\tau \sim 20$ s and $\tau \sim 40$ s at 0.5 cmc and 1 cmc, respectively. Compared to the lifetimes with air only, one sees that PFH has negligible effect at 0.5 cmc, but

that its presence leads to the a much broader distribution at the cmc, i.e. some of the films are significantly stabilized. Above the cmc, the average film lifetime is again constant with surfactant concentration, in line with those of films produced in air only. However longer average lifetimes are reached ($\tau \sim 90$ s) with again broader lifetime distributions.

In summary, we see without and with PFH the well-known influence of surfactant concentration on film stability: lifetimes increase with increasing surfactant concentration up to the cmc, beyond which they remain largely constant in the concentration range investigated. The PFH has a significant influence on the film lifetimes only above the cmc. As for the foam stability measurements, it seems that the full action of the PFH is fully exploited only when the surfactant monolayer is densely packed. We observe a broadening of the lifetimes in the presence of PFH which is expected from the scatter of the lifetime data shown in Figure 1b. We have no explanation for this observation jet.

Last but not least, the reader may wonder why the lifetimes of the foam films remain much lower than the lifetimes of the foams. This is due to the fact that the individual foam films in our experiments are not only much larger than those in the foams, which decreases their stability[37], but that the mechanism controlling the stability of vertical films is also slightly different, since they need to carry their own weight[38,39]. Moreover, the importance of evaporation on foam film rupture has been put in evidence lately[27,40]. While in foam bubbles the air is saturated with humidity (*RH* = 100%) in our foam film experiment we work in a range of *RH* = 75-85% leading to lower film stability.

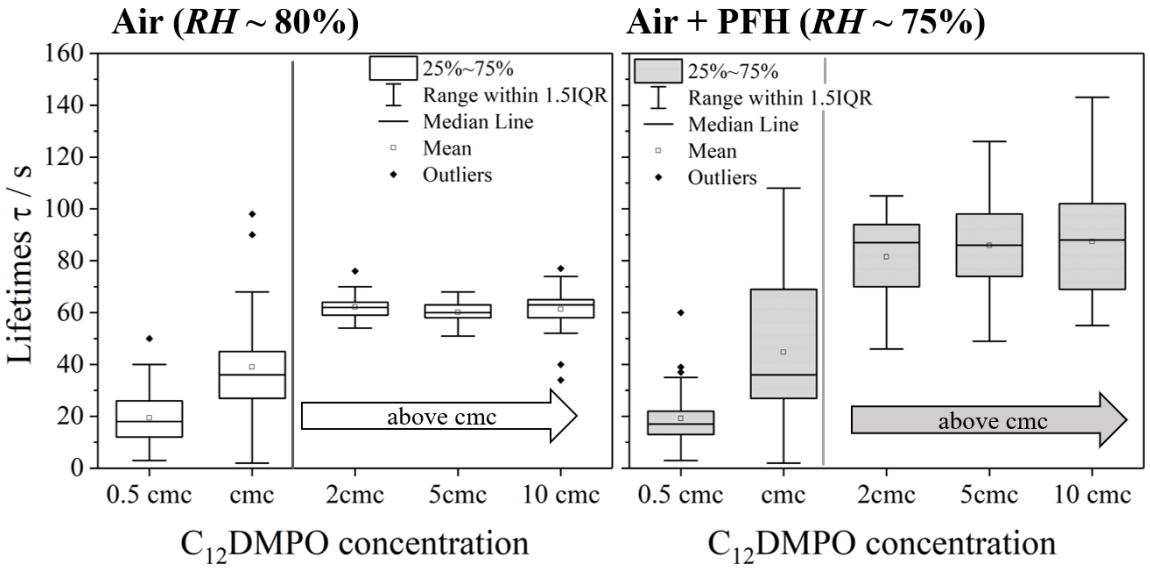

Figure 7: Box plot of the lifetimes of vertical foam films pulled from aqueous solutions of C_{12}DMPO at different concentrations (40 films per solution) without PFH (left) and with PFH (right) in the air surrounding the films. The relative humidity *RH* was kept constant at ~ 80% and ~ 75%, respectively. Each box reflects 50% of the data, with a lower quartile of 25%, the median line (50%) and an upper quartile of 75%, i.e. the smallest 25% (50%, 75% respectively) of the data

are lower or equal to the respective value. The range without outliers is set to 1.5 times the interquartile range (IQR).

3.4 Alkane Vapors

In the framework of our investigations it was interesting for us to see if alkane vapors have a similarly stabilizing influence on foams since they also co-adsorb to the interfaces. This comparison seemed particularly important , because Binks *et al.*[22] showed that alkane vapors are rather detrimental to foam stability. Figure 8a shows photographs of foams of aqueous C_{12}DMPO solutions at 10 cmc at increasing p/p_0 ratios of hexane in air, while Figure 8b plots the corresponding foam height h versus time t. In contradiction to Binks e*t al*., our measurements show an *increase* in foam stability with increasing alkane concentration. The initial foam heights obtained with the same gas volume increase with increasing presence of alkane vapor, indicating less coalescence during the foaming process. Moreover, the foams collapse less rapidly, once generated. We believe that this contrasting observation can be explained by different ways of inserting the alkane into the foaming gas. Binks *et al*. passed a nitrogen stream through successively arranged bubble counters containing liquid alkanes before introducing it into the surfactant solutions. Following this way, tiny alkane droplets might be taken along within the nitrogen stream, which, in turn, work as antifoamers leading to the lower foam stability. We prepared the air/alkane mixtures as described for the measurements with PFH, i.e. small volumes were filled in syringes filled with air such that the alkane evaporates immediately in the syringe. Thus, if we ensure that the alkane is present only in gaseous form, it actually *enhances* foam stability. Comparing the performance of hexane and perfluorohexane on slowing down coalescence in foams, one sees that alkanes are much less effective. Although the foam height decreases more slowly in the presence of hexane compared to the foam with air only, foam degradation is clearly visible. The foams at 300 s are more transparent than shortly after production, indicating a larger bubble size, hence a less effective slowing down of coalescence. In addition, hexane is much less effective in suppressing coarsening than PFH since at longer timescales, i.e. at 1000 s, the foams are collapsed to less than half their initial height. We recall that in the presence of PFH, the foam height and bubble size of foams of aqueous C_{12}DMPO at 10 cmc remained constant within the first 1000 s after foam production. The less effective suppression of coarsening can be explained by the higher solubility of alkanes in water.

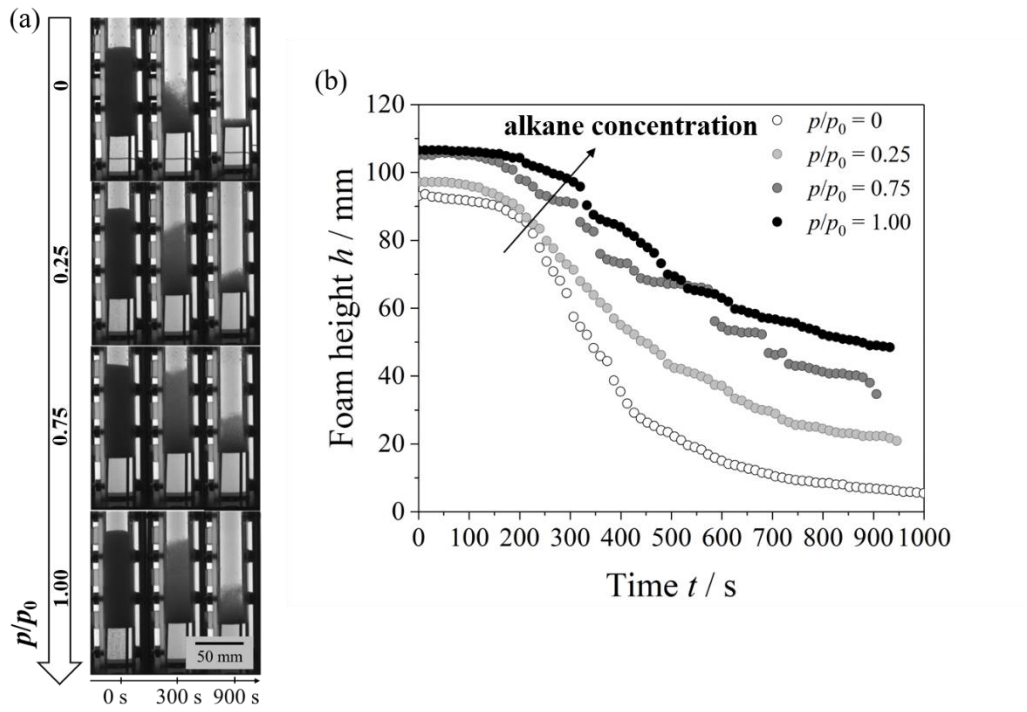

Figure 8: (a) Photographs of foams of aqueous C_{12}DMPO solutions at a concentration of c = 10 cmc with and without hexane in the foaming gas (air) taken during *FoamScan* measurements. The different concentrations of hexane are given by the ratio of the partial pressure p of hexane to its vapor pressure p_0. (b) Corresponding time evolution of the foam height h.

4. Discussion and conclusion

The present study provides confirmation that fluorocarbon vapors reduce coalescence in aqueous foams. Using the non-ionic surfactant C_{12}DMPO, we show that the impact of the PFH increases with increasing surfactant concentration and is fully developed once the surfactant monolayer is densely packed (above the cmc). We show that the same general tendencies hold for foams and for isolated foam films, the latter allowing to exclude the influence of coarsening.

The surface tension measurements confirm the co-adsorption of fluorocarbons to the interface, expressed by the reduction of the surface tension values in the presence of PFH[8,10,18]. We confirm furthermore, that at saturation of PFH (p/p_0 = 1), a macroscopically thick PFH film is formed on top of the surfactant monolayer. While the literature often talks about a true co-adsorption of the surfactant and the PFH, we want to stress here that the alkane tails of the surfactant monolayer and the PFHs are insoluble[6], i.e. the formation of a truly mixed layer is unlikely. It seems more likely that a PFH layer forms mostly "on top" of the surfactant monolayer with only slight interdigitation, as sketched in Figure 5II (< CMC) or 5V (> CMC), interfering probably with the organization of the surfactant monolayer. Below the CMC one may also imagine the formation of patchy layers alternating between zones of surfactant and PFH, as sketched in Figure5III. However, this would put the PFH into unfavorable direct contact with water and also likely lead to less stable foams due

to the presence of surfactant-free zones. While some attempts on modelling of this mixed layer were made[18] and some experimental investigations using neutron scattering were carried out[19], we believe that a scientifically sound molecular interpretation of the organization of this mixed layer is yet to be found. Molecular-scale simulations are probably the most promising tool at this stage to provide guidance.

In the same spirit, the precise mechanism why the co-adsorption of a surfactant and a fluorocarbon leads to a higher stability of the thin liquid films that separate two bubbles remains to be elucidated. Two possible explanations are (i) changes in the electrostatic, steric and van der Waals interactions (DLVO interactions) across the thin films[16,41] and/or (ii) changes in the viscoelastic behavior of the mixed layer. The latter, known to be affected by the presence of fluorocarbons[10,18], influences several processes in thin liquid films[41]. By fixing the boundary conditions, the viscoelastic behavior determines the characteristic drainage times of the thin films. It also provides a self-healing elasticity and thus counterbalances hole formation in the thin films due to local concentration gradients. It also has the capacity to hamper thermal fluctuations of the film thickness. FCs are known to fluidify strongly viscoelastic monolayers of lipids, proteins or polymers[8,10,11,18]. Could such a fluidification contribute to an increased stability of the Newton Black Film? On the contrary, the FCs may also rigidify the monolayers of the surfactant solutions at high surfactant concentrations. This could slow down film drainage, increase self-healing, and dampen thermal fluctuations. A rigidification of the interface could be explained by a "smectic-like" ordering of the fluorocarbon at the surfactant-covered interface, creating a "stabilizing shell" around the bubbles, hence slowing down coalescence. For water surfaces, a smectic-like ordering of FCs has been shown by Kashimoto et al.[42] using X-ray reflectivity measurements. For oil-based foams stabilized by lamellar layers around the bubbles, a similar mechanism has been reported[43–45].

The stabilization of foams against coalescence in the presence of a FC vapor could also be related to an increase of the energy required to create holes in the thin films which has been linked to the probability of rupture of foam or emulsion films[37,46,47]. This energy, dominated by surface tension, surface dilatational and/or surface bending elasticity, might be increased by the fluorocarbon, hence the probability of film rupture is lowered. Similar observations have also been made for emulsions[47], where the presence of traces of an insoluble molecular species has been observed to contribute greatly to a slowing down of coalescence, and not only coarsening, as had been originally expected. The authors explain this observation by the incompatibility of these molecules with the surfactant layer, leading to an osmotic effect which compacts the surfactant layer.

Last but not least, one may want to consider that the PFH adsorption may reduce water evaporation[38,39], as we observe in the final stage of film thinning. However, this evaporation is absent within the foams (the bubbles are saturated with water vapor (RH = 100%) and the foam cell is closed against evaporation). It seems therefore that the more important observation from the film investigations is the longer lifetime of the Newton Black Films.

In summary, the systematic observations of a reduced coalescence in foams produced from a wide range of surfactant systems in the presence of fluorocarbon vapors indicates a very robust

underlying phenomenon which still requires explanation. The fact, that similar observations are made in the presence of alkane vapors (Section 3.4), yet to a much lesser extent, seems to point towards the very peculiar nature of the fluorocarbon molecules. Future work therefore needs to identify clearly the molecular organization of the different species at the interface and their impact on the static and dynamic interfacial properties. Since our fundamental understanding of the mechanisms controlling foam stability even in the absence of FCs remains very limited[3,41,46,48], it is likely that a sound explanation of the influence of FC vapors on foam stability will remain an important challenge in future research. An interesting associated question will be to find alternatives to FCs with a similarly stabilizing effect. Globally, it is interesting to explore more systematically the idea of exploiting the co-adsorption of molecules from the gas phase for the control of foam stability.

Acknowledgement

The authors would like to thank Martin Hamann, Sébastien Andrieux, Dominique Langevin and Marie-Pierre Krafft for stimulating discussions. We thank Marie-Pierre Krafft to have shared numerous surfactants with us for preliminary tests (such as the F-PEG2000 shown in Figure S1 in the supporting information). Leandro Jacomine is thanked for help with the measurements. Cosima Stubenrauch acknowledges a fellowship by the Institute of Advanced Studies at the University of Strasbourg (USIAS), and Wiebke Drenckhan acknowledges financial support by an ERC consolidator grant (agreement 819511 - METAFOAM). Overall, this work was conducted in the framework of the Interdisciplinary Institute HiFunMat, as part of the ITI 2021-2028 program of the University of Strasbourg, CNRS and Inserm, was supported by IdEx Unistra (ANR-10-IDEX-0002) and SFRI (STRATUS project, ANR-20-SFRI-0012) under the framework of the French Investments for the Future Program.

Conflict of Interest

The authors declare no conflict of interest.

References

[1] I. Cantat, S. Cohen-Addad, F. Elias, F. Graner, R. Höhler, O. Pitois, F. Rouyer, A. Saint-Jalmes, R. Flatman, *Foams*, Oxford University Press, **2013**.

[2] R. J. Pugh, *Bubble and Foam Chemistry*, Cambridge University Press, Cambridge, **2016**.

[3] D. Langevin, *Emulsions, Microemulsions and Foams*, Springer International Publishing, Cham, **2020**.

[4] D. L. Weaire, S. Hutzler, *The Physics of Foams*, Clarendon Press, Oxford, **2001**.

[5] A. Kabalnov, D. Klein, T. Pelura, E. Schutt, J. Weers, *Ultrasound Med. Biol.* **1998**, *24*, 739–749.

[6] J. G. Riess, *Artif. Cells. Blood Substit. Immobil. Biotechnol.* **2005**, *33*, 47–63.

[7] K. Steck, M. Hamann, S. Andrieux, P. Muller, P. Kékicheff, C. Stubenrauch, W. Drenckhan, *Adv. Mater. Interfaces* **2021**, *8*, 10–15.

[8] V. B. Fainerman, E. V. Aksenenko, R. Miller, *Adv. Colloid Interface Sci.* **2017**, *244*, 100–112.

[9] F. Gerber, M. P. Krafft, T. F. Vandamme, M. Goldmann, P. Fontaine, *Angew. Chemie Int. Ed.* **2005**, *44*, 2749–2752.

[10] F. Gerber, M. P. Krafft, T. F. Vandamme, M. Goldmann, P. Fontaine, *Biophys. J.* **2006**, *90*, 3184–3192.

[11] L. Gazzera, R. Milani, L. Pirrie, M. Schmutz, C. Blanck, G. Resnati, P. Metrangolo, M. P. Krafft, *Angew. Chemie* **2016**, *128*, 10419–10423.

[12] Y. Ando, H. Tabata, M. Sanchez, A. Cagna, D. Koyama, M. P. Krafft, *Langmuir* **2016**, *32*, 12461–12467.

[13] B. P. Binks, D. Crichton, P. D. I. Fletcher, J. R. MacNab, Z. X. Li, R. K. Thomas, J. Penfold, *Colloids Surfaces A Physicochem. Eng. Asp.* **1999**, *146*, 299–313.

[14] V. B. Fainerman, E. V. Aksenenko, V. I. Kovalchuk, R. Miller, *Colloids Surfaces A Physicochem. Eng. Asp.* **2016**, *505*, 118–123.

[15] V. B. Fainerman, E. V. Aksenenko, S. V. Lylyk, Y. I. Tarasevich, R. Miller, *Colloids Surfaces A Physicochem. Eng. Asp.* **2017**, *521*, 211–220.

[16] V. B. Fainerman, E. V. Aksenenko, V. I. Kovalchuk, A. Javadi, R. Miller, *Soft Matter* **2011**, *7*, 7860–7865.

[17] A. Javadi, N. Moradi, V. B. Fainerman, H. Möhwald, R. Miller, *Colloids Surfaces A Physicochem. Eng. Asp.* **2011**, *391*, 19–24.

[18] M. P. Krafft, V. B. Fainerman, R. Miller, *Colloid Polym. Sci.* **2015**, *293*, 3091–3097.

[19] X. Liu, C. Counil, D. Shi, E. E. Mendoza-Ortega, A. V. Vela-Gonzalez, A. Maestro, R. A. Campbell, M. P. Krafft, *J. Colloid Interface Sci.* **2021**, *593*, 1–10.

[20] P. N. Nguyen, T. T. Trinh Dang, G. Waton, T. Vandamme, M. P. Krafft, *ChemPhysChem* **2011**, *12*, 2646–2652.

[21] H. Bey, F. Wintzenrieth, O. Ronsin, R. Höhler, S. Cohen-Addad, *Soft Matter* **2017**, *13*, 6816–6830.

[22] B. P. Binks, P. D. I. Fletcher, M. D. Haynes, *Colloids Surfaces A Physicochem. Eng. Asp.* **2003**, *216*, 1–8.

[23] J. Boos, W. Drenckhan, C. Stubenrauch, *J. Surfactants Deterg.* **2013**, *16*, 1–12.

[24] A. M. A. Dias, C. M. B. Gonçalves, A. I. Caço, L. M. N. B. F. Santos, M. M. Piñeiro, L. F. Vega, J. A. P. Coutinho, I. M. Marrucho, *J. Chem. Eng. Data* **2005**, *50*, 1328–1333.

[25] S. Andrieux, *Monodisperse Highly Ordered and Polydisperse Biobased Solid Foams*, Springer International Publishing, Cham, **2019**.

[26] L. Greenspan, *J. Res. Natl. Bur. Stand. - A. Phys. Chem.* **1977**, *81A*, 89–96.

[27] L. Champougny, J. Miguet, R. Henaff, F. Restagno, F. Boulogne, E. Rio, *Langmuir* **2018**, *34*, 3221–3227.

[28] R. Miller, E. V. Aksenenko, V. I. Kovalchuk, V. B. Fainerman, *Phys. Chem. Chem. Phys.* **2017**, *19*, 2193–2200.

[29] R. Miller, E. V. Aksenenko, V. I. Kovalchuk, Y. I. Tarasevich, V. B. Fainerman, *Physicochem. Probl. Miner. Process.* **2018**, *54*, 54–62.

[30] R. Miller, E. V. Aksenenko, V. I. Kovalchuk, D. V. Trukhin, Y. I. Tarasevich, V. B. Fainerman, *Adv. Mater. Interfaces* **2017**, *4*, DOI 10.1002/admi.201600031.

[31] M. G. Freire, P. J. Carvalho, A. J. Queimada, I. M. Marrucho, J. A. P. Coutinho, *J. Chem. Eng. Data* **2006**, *51*, 1820–1824.

[32] D. Grigoriev, C. Stubenrauch, *Colloids Surfaces A Physicochem. Eng. Asp.* **2007**, *296*, 67–75.

[33] L. Martínez-Balbuena, A. Arteaga-Jiménez, E. Hernández-Zapata, C. Márquez-Beltrán, *Adv. Colloid Interface Sci.* **2017**, *247*, 178–184.

[34] D. Blunk, R. Tessendorf, N. Buchavzov, R. Strey, C. Stubenrauch, *J. Surfactants Deterg.* **2007**, *10*, 155–165.

[35] S. Andrieux, M. Patil, L. Jacomine, A. Hourlier-Fargette, S. Heitkam, W. Drenckhan, *Macromol. Rapid Commun.* **2022**, *43*, DOI 10.1002/marc.202200189.

[36] E. Carey, C. Stubenrauch, *J. Colloid Interface Sci.* **2010**, *343*, 314–323.

[37] E. Forel, B. Dollet, D. Langevin, E. Rio, *Phys. Rev. Lett.* **2019**, *122*, 088002.

[38] L. Champougny, J. Miguet, R. Henaff, F. Restagno, F. Boulogne, E. Rio, *Langmuir* **2018**, *34*, 3221–3227.

[39] L. Champougny, E. Rio, F. Restagno, B. Scheid, *J. Fluid Mech.* **2017**, *811*, 499–524.

[40] F. Boulogne, F. Restagno, E. Rio, *Phys. Rev. Lett.* **2022**, *129*, 268001.

[41] E. Rio, A.-L. Biance, *ChemPhysChem* **2014**, *15*, 3692–3707.

[42] K. Kashimoto, J. Yoon, B. Hou, C. H. Chen, B. Lin, M. Aratono, T. Takiue, M. L. Schlossman, *Phys. Rev. Lett.* **2008**, *101*, DOI 10.1103/PhysRevLett.101.076102.

[43] S. E. Friberg, Chang Sup Wohn, B. Greene, R. Van Gilder, *J. Colloid Interface Sci.* **1984**, *101*, 593–595.

[44] S. E. Friberg, I. Blute, H. Kunieda, P. Stenius, *Langmuir* **1986**, *2*, 659–664.

[45] S. E. Friberg, I. Blute, P. Stenius, *J. Colloid Interface Sci.* **1989**, *127*, 573–582.

[46] D. Langevin, *Adv. Colloid Interface Sci.* **2020**, *275*, 102075.

[47] H.-H.-Q. Dinh, E. Santanach-Carreras, M. Lalanne-Aulet, V. Schmitt, P. Panizza, F. Lequeux, *Langmuir* **2021**, *37*, 8726–8737.

[48] D. Langevin, *Curr. Opin. Colloid Interface Sci.* **2019**, *44*, 23–31.

Supporting Information

Fluorocarbon Vapors Slow Down Coalescence in Foams: Influence of Surfactant Concentration

Katja Steck[1], Jonathan Dijoux[1], Natalie Preisig[2], Victor Bouylout[1], Cosima Stubenrauch[2], Wiebke Drenckhan[1]

[1]Institut Charles Sadron, University of Strasbourg, CNRS UPR22, 23 Rue du Loess, 67037 Strasbourg, France

[2]Institute of Physical Chemistry, University of Stuttgart, Pfaffenwaldring 55, 70569 Stuttgart, Germany

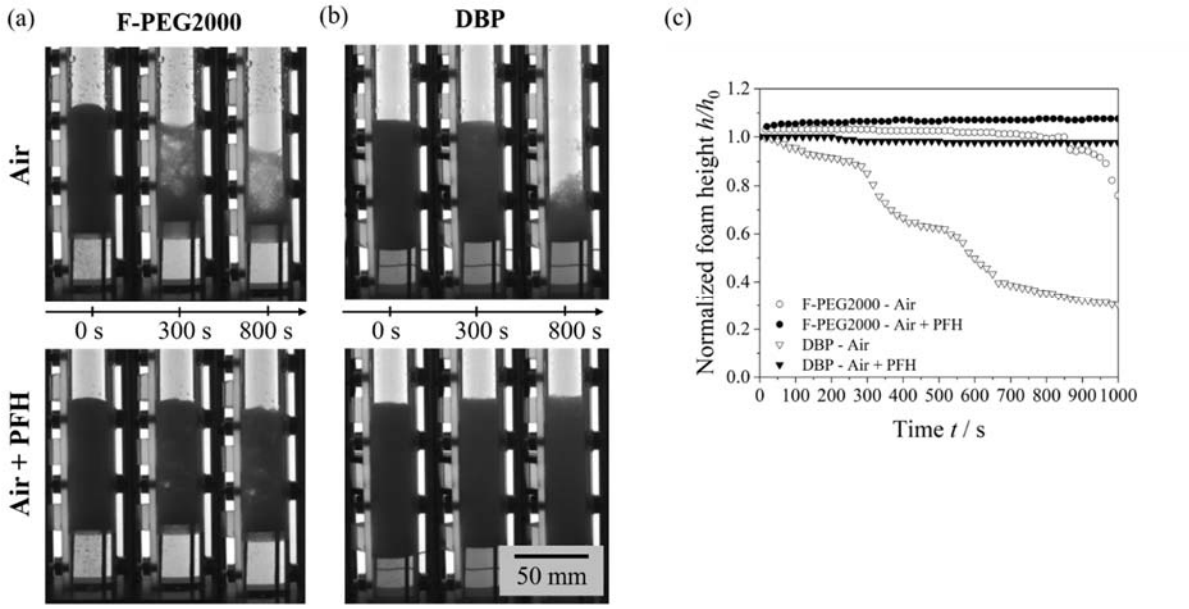

Figure S1: Photographs of foams of aqueous solutions of (a) fluorinated poly(ethylene glycol) 2000 (F-PEG2000) and (b) a dimethylsiloxane block copolymer (DBP732) at c = 10 cmc with and without perfluorohexane (PFH) in the foaming gas (air) taken during *FoamScan* measurements. The amount of PFH, i.e. the ratio of partial pressure p of perfluorohexane to its vapor pressure p_0, was set to $p/p_0 = 0.15$. (c) Corresponding normalized foam height h/h_0 versus time t curves.

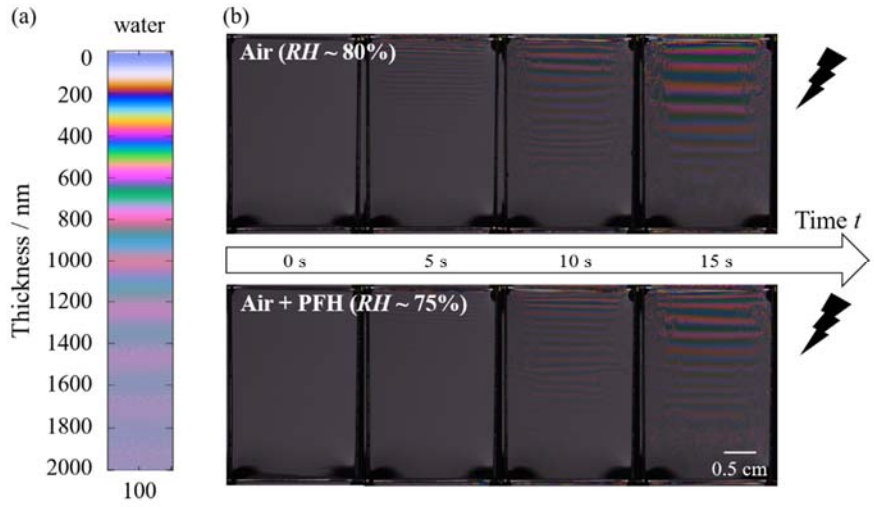

Figure S2: (a) Color code related to the thickness of a draining vertical thin film of an aqueous solution and (b) evolution of drainage of vertical thin films of an aqueous C_{12}DMPO solution at 0.5 cmc in the absence and presence of PFH in the measuring chamber of the film pulling device with relative humidity *RH*.

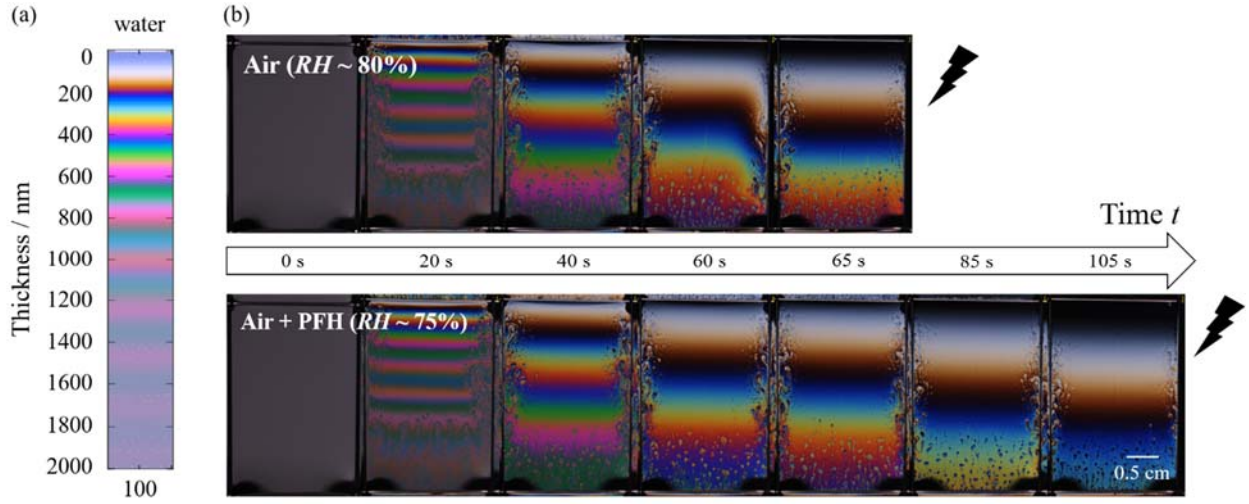

Figure S3: (a) Color code related to the thickness of a draining vertical thin film of an aqueous solution and (b) evolution of drainage of vertical thin films of an aqueous C_{12}DMPO solution at 2 cmc in the absence and presence of PFH in the measuring chamber of the film pulling device with relative humidity *RH*.